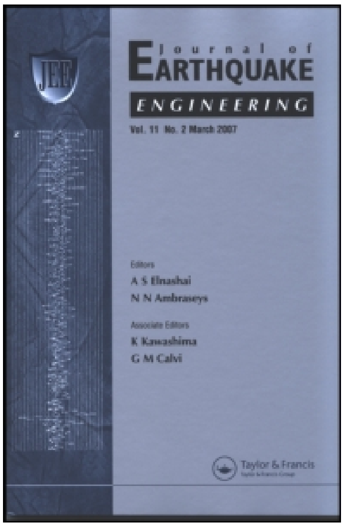


**Journal of Earthquake Engineering**
Publication details, including instructions for authors and subscription information:
http://www.informaworld.com/smpp/title~content=t741771161

# Approximate Methods for Estimating Hysteretic Energy Demand on Plan-Asymmetric Buildings

Manish Rathore[a]; Amarnath Roy Chowdhury[a]; Siddhartha Ghosh[a]
[a] Department of Civil Engineering, Indian Institute of Technology Bombay, Mumbai, India

Online publication date: 06 January 2011

**To cite this Article** Rathore, Manish , Chowdhury, Amarnath Roy and Ghosh, Siddhartha(2011) 'Approximate Methods for Estimating Hysteretic Energy Demand on Plan-Asymmetric Buildings', Journal of Earthquake Engineering, 15: 1, 99 — 123

**To link to this Article: DOI:** 10.1080/13632461003681163
**URL:** http://dx.doi.org/10.1080/13632461003681163

*Journal of Earthquake Engineering*, 15:99–123, 2011

ISSN: 1363-2469 print / 1559-808X online
DOI: 10.1080/13632461003681163

# Approximate Methods for Estimating Hysteretic Energy Demand on Plan-Asymmetric Buildings

MANISH RATHORE, AMARNATH ROY CHOWDHURY, and SIDDHARTHA GHOSH

Department of Civil Engineering, Indian Institute of Technology Bombay, Mumbai, India



*The first step in a hysteretic energy-based design approach of performance-based design is the estimation of hysteretic energy demand in the structure. A nonlinear response-history analysis of the multi-degree of freedom model gives an accurate estimation, but it is not suitable for adopting in design. Two alternative methods, based on the concepts of modal pushover analysis (MPA) and 2D-MPA, are proposed in this article for uniaxial plan-asymmetric structures. Application studies show that both methods are efficient. While the 2D-MPA-based method is more accurate, the MPA-based method is more suitable for design adoption. Significant conclusions are given for prospective application of these methods.*

**Keywords** Hysteretic Energy Demand; Asymmetric Structures; Modal Pushover Analysis; 2D-MPA; Energy-Based Design

## 1. Introduction

The general philosophy for earthquake-resistant design of structures has undergone some major changes in the past 15 years, following some of the most devastating earthquakes all over the world. The conventional elastic force-based design methodology using (design) acceleration spectra is gradually getting replaced by more rational seismic design approaches. The primary focus of these advanced approaches is in a realistic characterization of seismic structural damage and its direct incorporation in the design methodology. In addition, a major emphasis is given to the characterization of all the uncertainties in the process of design (or, lifecycle engineering, for more advanced design approaches). In general, these approaches are categorized under performance-based seismic design (PBSD). The various ways of modeling structural damage for PBSD lead to various design approaches. The most commonly adopted approach for PBSD so far is the displacement-based design approach, where the design criterion is set usually by a limit on the peak roof (inelastic) displacement, the peak (inelastic) inter-story drift, or the peak ductility demand, etc. However, many researchers argued that the cumulative energy dissipated due to cyclic-plastic deformations occurring in a structure (that is, the hysteretic energy) is directly related to seismic damage in structures [Zahra and Hall, 1984; Fajfar, 1992; Manfredi, 2001]. The argument provided in favor of considering the hysteretic energy demand as design criterion is that it can directly account for the cumulative nature of damage in the structure and the dynamic nature of earthquake.

Received 13 June 2009; accepted 5 February 2010.
Address correspondence to Siddhartha Ghosh, Department of Civil Engineering, Indian Institute of Technology Bombay, Powai, Mumbai 400076, India; E-mail: sghosh@civil.iitb.ac.in

The necessity of an energy-based design procedure for future seismic design guidelines has been emphasized by many researchers, including a few attempts at providing a framework for such design procedures. Discussions of these efforts can be found in Ghosh and Collins [2006] and Prasanth *et al.* [2008]. The first significant step in a hysteretic energy-based design is the estimation of hysteretic energy demand due to the design ground motion scenario. With the computing facilities available today, this estimation for a specific structure under a certain earthquake ground motion is not difficult, although it is computation intensive. However, one has to apply this detailed method—nonlinear response history analysis (NLRHA) of a multi-degree of freedom (MDOF) model—for each individual structure separately, making this direct method unsuitable for incorporating in a general purpose design methodology based on hysteretic energy demand. Thus, it becomes necessary to use some approximate method for estimating the energy demand that can be easily incorporated in seismic design codes. Such a method will also be useful for the energy-based performance assessment/evaluation of existing structures and for the purpose of energy-based design checking. Prasanth *et al.* [2008] used a modal pushover analysis- or MPA-based [Chopra and Goel, 2002] approximate method to estimate the hysteretic energy demand in a structure when it is subjected to an earthquake ground motion. Although their method was limited only to symmetric-in-plan building structures, the results obtained for three such framed structures subjected to various earthquake scenarios were satisfactory and the method was deemed suitable for adopting in energy-based design and evaluation guidelines since it could use hysteretic energy response spectra.



The primary objective of this article is to propose an extension of the method proposed by Prasanth *et al.* [2008] to the hysteretic energy demand ($E_h$) estimation for (uniaxial) plan-asymmetric building structures and to validate these with various case studies. Two new methods for plan-asymmetric frame structures, following the concepts of MPA for asymmetric structures [Chopra and Goel, 2004] and 2D-MPA for uniaxial asymmetric systems [Lin and Tsai, 2007], are investigated here. Both the methods are based on developing modal equivalent systems for the original structure and obtaining the energy demand on this structure from the demands estimated on its equivalent systems. Brief overviews of the methods proposed for asymmetric structures by Chopra and Goel [2004] and Lin and Tsai [2007] are presented in Sec. 2. This section also includes an overview of the method proposed by Prasanth *et al.* [2008]. Sections 3 and 4 provide the proposed methodologies for the hysteretic energy demand estimation using the MPA and the 2D-MPA methods, respectively. The proposed methods are validated through the $E_h$ estimation for three building structures of low-to-high-rise configurations and also for different values of the plan eccentricity, under various earthquake scenarios. A detailed case study with statistical analysis of bias for each of the proposed estimation methods is provided in Sec. 5. These case studies are the primary focus of the work presented here, as these show the wide range of applicability of the methods proposed and also the variation in the accuracy of the estimation under various building configurations and earthquake scenarios. Section 6 discusses a few important observations based on these two case studies. Section 7 presents a sample case study of application of the two methods for a "torsionally flexible" structure as opposed to the "torsionally stiff" structures considered in Secs. 5 and 6. Significant conclusions based on this work are presented in Sec. 8.

## 2. Previous Related Research Works

The necessity of an energy-based seismic design was first proposed five decades ago by Housner [1956]. Since then, many researchers, such as Zahra and Hall [1984], Uang and Bertero [1988], and Fajfar [1992] emphasized the need of using the hysteretic energy demand as damage measure in seismic design and performance evaluation guidelines. Few design methodologies were also proposed trying to incorporate hysteretic energy or similar parameters as the measure of damage [Fajfar and Gašperešič, 1996; Ghosh and Collins, 2006]. Equivalent system alternatives for estimating the hysteretic energy demand were also proposed in these works. Although those methods worked well for the $E_h$ estimation in low-rise buildings, they failed in providing good estimates for the high-rises [Ghosh and Collins, 2006]. It was suspected that the single equivalent single degree of freedom (ESDOF) representation, used in these works, could not take into account the higher-mode effects, as the ESDOF system was primarily based on the fundamental mode of the original multi-degree of freedom (MDOF) structure. This limitation became prominent for the mid-to-high-rise structures where a greater participation of the higher modes is usually expected.

The modal pushover analysis (MPA) method was first proposed by Chopra and Goel [2002], as an approximate alternative to the nonlinear response-history analysis (NLRHA), for estimating peak force and displacement responses of symmetric structures using multiple pushover analyses. Each nonlinear static pushover analysis corresponded to a specific mode of vibration of the original structure using a lateral force distribution based on the corresponding mode shape vector. The peak structural (force and displacement) responses were obtained by combining the results from these modal pushover analyses. The method was tested on the SAC steel moment frame buildings from Los Angeles under several ground motion scenarios, and responses (peak displacement, maximum interstory drift, story shear, etc.) based on MPA are compared with those from the NLRHA. The results based on MPA were found to be satisfactory. These included both linear and nonlinear structural behaviour and cases where the higher mode effects were not negligible. The MPA method for symmetric structures was later extended to plan-asymmetric structures [Chopra and Goel, 2004]. The difference in this method from the previous was that, for the modal pushover analysis in each mode, the force vector included a moment (about the vertical axis) in addition to the lateral force at each story. Similar to the method proposed for symmetric structures, the force vector for asymmetric systems was also a linear function of the corresponding mode shape vector which included both lateral and rotational elements. The other important difference was that two pushover curves were available for each mode corresponding to the two orthogonal horizontal roof displacements, of which Chopra and Goel recommended the use of the curve corresponding to the dominant displacement direction for that mode. The modified method was tested on the 9-story SAC building from Los Angeles, but with an assumed 10% eccentricity in the longer direction. They also tested this method for different degrees of coupling between the lateral and the torsional modes by varying the rotational to lateral mass ratio similarly at all floors. It was concluded from their work that the MPA method gives equally good results for torsionally stiff and torsionally flexible uniaxial plan-asymmetric structures, but the accuracy decreases for torsionally equally flexible asymmetric structures.

An improved method following the basic concepts of MPA was later proposed by Lin and Tsai [2007] for the analysis of uniaxial plan-asymmetric buildings, known as the 2D-MPA method. This method also uses multiple modal pushover based equivalent systems to represent the original structure, however each modal equivalent system is a two degrees of freedom (2-DOF) system in this method. Lin and Tsai used both base shear versus roof displacement and base torque versus roof rotation pushover curves in this method. They noted that due to the coupling between lateral and torsional modes, the modal translation and modal rotation of floors were not proportional when the system deformed into the inelastic state. This opposed an implicit assumption made by Chopra and Goel [2004] while using an equivalent single degree of freedom system for asymmetric structures. The modal equivalent system proposed by Lin and Tsai has two degrees of freedom representing translational and rotational movements in each mode. These equivalent 2-DOF systems can take into account the bifurcating nature of modal translations and rotations because these are formulated considering both the base shear versus roof translation and base torque versus roof rotation pushover curves. Lin and Tsai tested this method on a two-story structure and the results (displacement demands on various floors) were more accurate (that is, closer to results from NLRHA) as compared to those using the ESDOF-based MPA method.

Prasanth *et al.* [2008] used the concepts of MPA method proposed by Chopra and Goel [2002] to estimate hysteretic energy demands on symmetric-in-plan structures. Here, the properties of modal equivalent single degree of freedom systems were obtained based on the nonlinear static modal pushover curves. A nonlinear response history analysis of a modal ESDOF system gave the modal hysteretic energy demand. The hysteretic energy demand on the structure was obtained by summing up the modal hysteretic energy demands for various modes. The proposed method was tested on the 3-, 9-, and 20-story SAC buildings from Los Angeles, which represented typical low-, medium-, and high-rise structures, subjected to various strong motion scenarios. These results were compared with those obtained from NLRHA and by Ghosh and Collins [2006] using a nonlinear pushover-based single equivalent system. The method was found to be very effective, and more accurate than the method proposed by Ghosh and Collins, in estimating hysteretic energy demand in structures. Prasanth *et al.* also recommended that even for high-rise structures, consideration of only the first three modes is sufficient for estimating the structure's energy demand. In the present work, the method proposed by Prasanth *et al.* for estimating hysteretic energy demand is extended to uniaxial plan-asymmetric structures by using the concepts of both the MPA and the 2D-MPA methods for asymmetric systems.



## 3. Estimation of $E_h$ using the MPA-Based Method

The basic method adopted here in estimating the hysteretic energy demand follows the method proposed by Prasanth *et al.* [2008] using the concepts of MPA [Chopra and Goel, 2004]. The basic concepts are discussed in the previous section, and this section provides a step-wise methodology for this estimation.

The individual steps of the proposed method are:

1. Create an analytical model of the actual structure suitable for nonlinear static and dynamic analyses. The lumped mass matrix **M** of the structure contains both the mass (**m**) and moment of inertia ($\mathbf{I}_0$) submatrices corresponding to one translational and one rotational degrees of freedom, respectively, at each floor:

$$\mathrm{M} = \begin{bmatrix} \mathbf{m} & \mathbf{0} \\ \mathbf{0} & \mathbf{I}_0 \end{bmatrix}_{2N \times 2N}. \tag{1}$$

   $N$ is the number of floors where the masses are lumped.

2. Perform an eigenvalue analysis to obtain the natural periods and mode shapes for each mode: $T_n$ = natural period of the $n$th mode and $\boldsymbol{\varphi}_n$ = $n$th mode shape vector, normalized to $M_n$ = 1, where $M_n$ is the modal mass for the $n$th mode:

$$\mathrm{M}_n = \boldsymbol{\varphi}_n^{\mathrm{T}} \mathbf{M} \boldsymbol{\varphi}_n. \tag{2}$$

The mode shape vector contains both translational (denoted with $x$) and rotational (denoted with $\theta$) elements:

$$\boldsymbol{\varphi}_n = \begin{Bmatrix} \boldsymbol{\varphi}_{xn} \\ \boldsymbol{\varphi}_{\theta n} \end{Bmatrix}_{2N\times 1}. \tag{3}$$

3. Calculate the modal participation factor ($\Gamma_n$) for the $n$th mode as:

$$\Gamma_n = \frac{\boldsymbol{\varphi}_n^T \mathbf{M}\boldsymbol{\iota}}{\boldsymbol{\varphi}_n^T \mathbf{M}\boldsymbol{\varphi}_n}. \tag{4}$$

   where $\boldsymbol{\iota}$ represents the influence vector.
4. Perform a modal pushover analysis for the $n$th mode, using the lateral force (and moment) distribution $\mathbf{f}_n = \mathbf{M}\boldsymbol{\varphi}_n$. Continue this analysis until a maximum interstory drift of 2.5% is reached.
5. Approximate the base shear ($V_{bn}$) versus roof displacement ($u_{rn}$) "pushover" curve with a bilinear one, by equating the areas underneath the original and the approximate curves [Ghosh and Collins, 2006; Prasanth *et al.*, 2008]. Obtain the initial (elastic) stiffness ($K_{in}$), the yield displacement ($D_{yn} = V_{bny}/K_{in}$, where $V_{bny}$ is the yield base shear of the structure), and the strain-hardening stiffness ratio ($\alpha_{kn}$) from the bilinear approximation.
6. The $n$th modal ESDOF system's mass and stiffness properties ($M_n$, elastic stiffness $K_{xn}$, yield displacement $D_{ny}$, yield force $V_{ny}$, and $\alpha_{kn}$) are obtained from these modal pushover results similar to the work of Prasanth *et al.* For example, the elastic stiffness of the ESDOF system is calculated as $K_{xn} = K_{in}\boldsymbol{\varphi}_n{}^{\mathrm{T}}\mathbf{f}_n$. Using these parameters the nonlinear hysteretic force-deformation relationship $G(q_n)$ for equivalent system [Prasanth *et al.*, 2008] is obtained.
7. The $n$th modal equivalent system is solved for the selected acceleration time-history ($\ddot{u}_g$) using a nonlinear response-history analysis:

$$\ddot{q}_n + 2\zeta_n\omega_n q_n + \omega_n^2 G(q_n) = -\Gamma_n \ddot{u}_g(t), \tag{5}$$

   where $q_n$ is the modal displacement for the $n$th mode, and $G(q_n)$ is a function describing the nonlinear force-deformation behaviour of the $n$th modal ESDOF.
8. Obtain the modal hysteretic energy demand ($E_{nh}$) at the end of the earthquake duration based on this solution. Simple user-friendly computer packages, such as NONLIN [Charney, 1999], can be used for this. If nonlinear hysteretic energy response spectrum is available for the selected record, that can also be used as an alternative.
9. Obtain the hysteretic energy demand on the structure ($E_{MPA}$) by adding the modal energy demands for the significant modes.

It should be noted here that the pushover plot which is used for obtaining the ESDOF system parameters is the one corresponding to the dominant displacement direction (between the two horizontal degrees of freedom at each floor) for that mode. For each mode, the pushover analysis is carried out to a maximum interstory drift of 2.5%. This is as per the suggestion made in previous works [Prasanth *et al.*, 2008; Ghosh and Collins, 2006]. Although there is no theoretical basis in adopting this limiting drift value, it is observed here, as in the earlier cases, that the change in the ESDOF parameters for considering other (higher) values of maximum interstory drift is insignificant. Prasanth *et al.* recommended computing the modal energy demands only from the first three modes' equivalent systems. Following the same concept, the first six modal equivalent systems (however, not more than three primarily translational and three primarily rotational modes) are considered for the case studies presented herein. Since $E_{nh}$ is a cumulative function in time, the peak hysteretic energy always occurs at the end of the analysis. The structural energy demand ($E_{MPA}$) is obtained by simply adding up the modal contributions of energy. However, this is still an approximation because it ignores any possible coupling in between modes in the inelastic domain as explained in the work by Prasanth *et al.* [2008].

## 4. Estimation of $E_h$ using the 2D-MPA-Based Method

The 2D-MPA method [Lin and Tsai, 2007] is similar to the MPA method in some aspects, with the primary difference that each equivalent system used here to evaluate the modal contribution has two degrees of freedom. Concepts of the 2D-MPA method are used here to extend the approximate hysteretic energy demand estimation technique proposed by Prasanth *et al.* [2008] to plan-asymmetric structures. Following, is a step-wise description of the 2D-MPA-based method for hysteretic energy demand. The first four steps remain the same as those for the MPA-based method presented in the previous section.

5. Obtain the base shear ($V_{bn}$) vs. roof displacement ($u_{rn}$) pushover curve and the base torque ($T_{bn}$) vs, roof rotation ($\theta_{rn}$) pushover curve for each mode.
6. Convert these pushover plots into the "acceleration-displacement response spectrum" or ADRS format [Lin and Tsai, 2007]:

$$\begin{aligned} A_{xn} &= \frac{V_{bn}}{\Gamma_{xn}^2 M_n}; A_{\theta n} = \frac{T_{bn}}{\Gamma_{\theta n}\Gamma_{xn} M_n} \\ D_{xn} &= \frac{u_{rn}}{\Gamma_{xn}\phi_{rxn}}; D_{\theta n} = \frac{\theta_{rn}}{\Gamma_{xn}\phi_{r\theta n}}, \end{aligned} \tag{6}$$

   where, $A_{xn}$ and $A_{\theta n}$ are the $n$th modal "accelerations" in the translational and rotational directions, respectively. $D_{xn}$ and $D_{\theta n}$ are the corresponding "displacement" functions in pushover curves in the ADRS format.
7. Bilinearize these plots similar to the MPA-based method. Obtain the initial stiffnesses ($K_{ixn}$ and $K_{i\theta n}$), yield accelerations ($A_{yxn}$ and $A_{y\theta n}$), and strain-hardening stiffness ratios ($\alpha_{xn}$ and $\alpha_{\theta n}$) from the two pushover plots.
8. Using the above parameters, obtain the $n$th modal equivalent 2-DOF system's properties following Eqs. (26), (48), and (49) in Lin and Tsai [2007]. For the $n$th modal equivalent system, these properties include: initial stiffnesses ($K_{xn}$ and $K_{\theta n}$), post-to-pre-yield stiffness ratios ($\alpha_{xn}$ and $\alpha_{\theta n}$), yield forces for the springs ($F_{yxn}$ and $F_{y\theta n}$), translational mass ($m$), and moment of inertia ($I_0$) of the lumped mass, eccentricity for the mass ($e$), etc. For example, $m$ and $I_0$ are calculated as:

$$m = \boldsymbol{\varphi}_{xn}^{\mathrm{T}} \mathbf{m} \boldsymbol{\varphi}_{xn}; I_0 = \boldsymbol{\varphi}_{\theta n}^{\mathrm{T}} \mathbf{I}_0 \boldsymbol{\varphi}_{\theta n} \tag{7}$$

   and the spring yield forces are obtained from these parameters:

$$F_{yxn} = A_{yxn} m; F_{y\theta n} = A_{y\theta n} I_0. \tag{8}$$

9. The $n$th modal equivalent 2-DOF system is solved for the selected acceleration time history ($\ddot{u}_g$) using a nonlinear response-history analysis.
10. Obtain the modal hysteretic energy demand ($E_{nh}$) based on this analysis.
11. Obtain the hysteretic energy demand on the structure ($E_{2D\text{-}MPA}$) by adding the modal energy demands for the significant modes.

It should be noted that the stiffness matrix **K** for the original structure is obtained by inverting its flexibility matrix, where the flexibility matrix is obtained by performing unit load static analysis for one degree of freedom at a time and calculating the displacements for each of them. The translational and rotational pushover plots give the same initial slope when converted into the ADRS format, however the strain-hardening stiffness ratios are different. No user-friendly software such as NONLIN is available to the general user to perform the nonlinear response-history analysis of a two degrees of freedom system. In order to use the commonly preferred structural analysis programs like OpenSees [Mazzoni *et al.*, 2007] or DRAIN-2DX [Prakash *et al.*, 1993], an alternative equivalent 2-DOF system is proposed here. The proposed equivalent system (Fig. 1a) is easier to use than that proposed by Lin and Tsai [2007] (Fig. 1b), because:

- a planer 2-DOF system is used instead of a 3-dimensional model;
- all the rotational (stiffness) springs are replaced by translational springs;
- no "zero-length element" is needed to model this system.

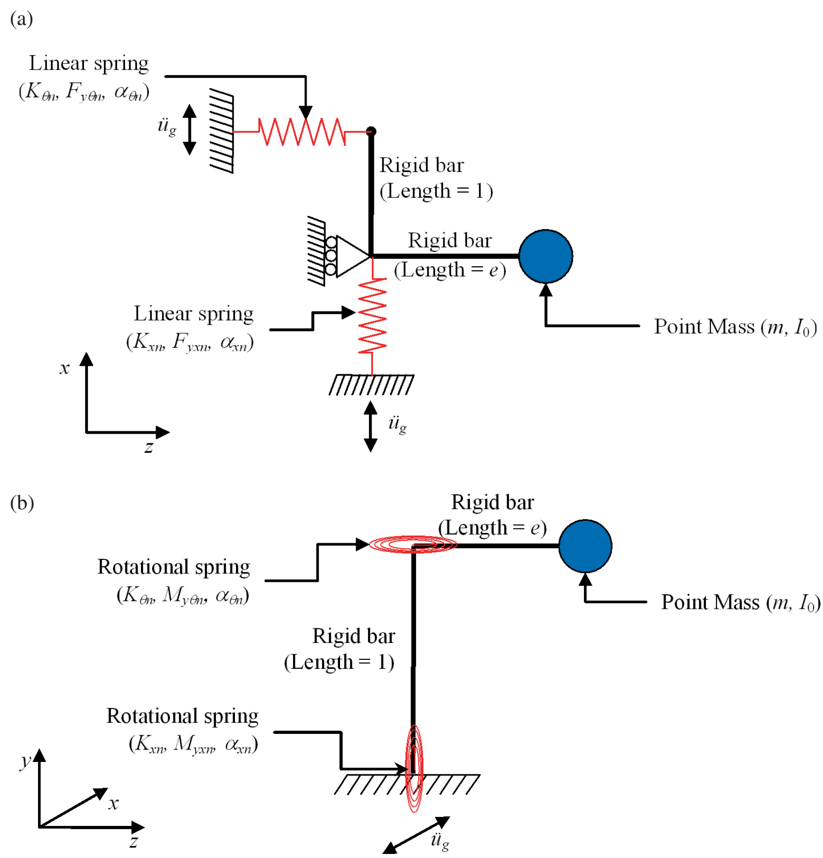


**FIGURE 1** 2-DOF modal equivalent systems (a) proposed in this article, and (b) proposed by Lin and Tsai [2007]. (Figure is provided in color online.)

The proposed system is validated by comparing response time histories with the system proposed by Lin and Tsai, subjected to the same ground motion records. The modal hysteretic energy demand on this system for a selected ground acceleration is obtained by applying a simple integrating scheme to the force and displacement time-histories of the two springs. Similar to the MPA-based method, modal contributions for the first 6 modes (but not more than the first three primarily translational and the first three primarily rotational modes) are added to calculate $E_{2D\text{-}MPA}$.

## 5. Application of the MPA-Based and 2D-MPA-Based Methods

The effectiveness of the two approximate energy estimation methods described in the previous two sections is tested by applying the proposed methods to estimate the hysteretic energy demands on three (3-, 9-, and 20-story) steel moment-framed buildings subjected to 18 different seismic ground motion records. These estimates are compared with the demands obtained from nonlinear response-history analyses of the MDOF system ($E_{NLRHA}$). The three buildings considered here are modified versions of the three "pre-Northridge" SAC steel buildings from Los Angeles. CA, details for which (dimensions, sections, loads, etc.) can be found in various documents, such as Gupta and Krawinkler [1999], and is avoided in this article. It should be noted, however, that the application of the proposed energy estimation procedures is neither limited to steel structures, nor to moment frames. These buildings are selected for this case study because they represent standard earthquake resistant designs and were used in various research studies, including an application of MPA on asymmetric systems by Chopra and Goel [2004]. These originally symmetric-in-plan buildings are changed to uniaxial plan-asymmetric buildings by shifting the center of mass at floor levels. The magnitude and direction of eccentricity introduced remain the same for all floors. The proposed methods are tested on these structures for different values of eccentricity in order to check their applicability for different degrees of asymmetry. For each of the three buildings, the following eccentricities (expressed as percentage of the building dimension along the direction of eccentricity) are considered in order to cover a wide range from symmetric to highly asymmetric structures: 0%, 5%, 10%, 20%, 30%, and 40%. Seismic ground motions are applied perpendicular to the direction of eccentricity so that the buildings have torsional motions. These are the same 18 strong motion records used by Prasanth *et al.* [2008] for the validation of their MPA-based method for symmetric buildings.

The NLRHA of the MDOF systems is performed using the open-source structural analysis software OpenSees [Mazzoni *et al.*, 2007]. Beams and columns are modeled using the nonlinear beam-column element with fiber section plastic hinges and five integration points in each element. The material is assumed to be elastic-perfectly plastic steel with members having a hysteretic (moment-curvature/force-deformation) behavior without any strength or stiffness degradation. Previous researchers [Kunnath *et al*., 1997; Erberik and Sucuoğlu, 2004] pointed out that the demand is very different for a system with pinched hysteretic behavior compared to that without any deterioration in subsequent deformation cycles. Thus, the findings of this work cannot be generally applied to deteriorating/pinched hysteretic systems. The rigid floor diaphragm effect is considered at all floor levels. A 5% Rayleigh damping is considered for the first two primarily lateral modes. Geometric nonlinearities in terms of the P-$\Delta$ and P-$\delta$ effects are not considered for any analysis. The NLRHA of the equivalent 2-DOF systems are also performed in OpenSees, where the translational springs are modeled with nonlinear truss elements. Detailed information on all the structural (and statistical) analyses and their outcomes are

**TABLE 1** Some properties of the first three modal ESDOF systems of the 9-story building with 10% eccentricity used in the MPA-based method

| Mode $n$ | $M_n$ (kNs$^2$/m) | $K_{xn}$ (kNm) | $\alpha_{kn}$ | $V_{ny}$ (kN) | $T_n$ (s) |
|---|---|---|---|---|---|
| 1 | 1.00 | 0.975 | 1.63E–01 | 2540 | 2.14 |
| 2 | 1.00 | 3.01 | 1.68E–01 | 4580 | 1.22 |
| 3 | 1.00 | 6.93 | 1.52E–01 | 4460 | 0.802 |

available in Rathore [2009]. As an example, some important ESDOF properties for the first three modes of the 9-story structure with 10% eccentricity used in the MPA-based method and those of the first three modal 2-DOF systems of the same structure used in the 2D-MPA-based method are presented in Tables 1 and 2, respectively.

The accuracy of a proposed approximate energy estimation method is measured using the statistics of a bias factor defined as:

$$N_{MPA} = \frac{E_{NLRHA}}{E_{MPA}}; N_{2D-MPA} = \frac{E_{NLRHA}}{E_{2D-MPA}}. \tag{9}$$

The approximate method gives an ideal estimate when this bias is equal to 1. A bias greater than 1 signifies an underestimation of the actual hysteretic energy demand by an approximate procedure. For a selected building with certain eccentricity, the bias factor is calculated for each earthquake and various statistical parameters—mean, standard deviation (SD), coefficient of variation (CoV) and absolute maximum error expressed as percentage (MaxEr)—are calculated for all 18 records. The bias factor statistics for three sample structures (with different heights and plan eccentricity) along with energy estimates for individual earthquakes are presented in Tables 3–5 for both the MPA-based and 2D-MPA-based methods. The $N_{MPA}$ and $N_{2D\text{-}MPA}$ statistics for all the case studies are summarily presented in Tables 6 and 7, respectively. Tables 8–10 give the modal contributions of energy for the MPA-based method for the same sample case studies as in Tables 3–5. The individual modal contributions are expressed as percentage of the $E_{MPA}$ considering upto 5 modes (the 6th mode is the 4th primarily translational mode, and also it does not contribute to the energy demand). Similar information for the same sample structures and for the 2D-MPA-based method are presented in Table 11–13.

The accuracy of estimates is also studied using simple scatterplots that provide an easy measure of how efficient an approximate method is. Figures 2–4 present scatterplots for the 3-, 9-, and 20-story buildings, respectively. These are plots of the hysteretic energy demand estimated by an approximate method ($E_{MPA}$ or $E_{2D\text{-}MPA}$) versus the energy estimated by the accurate method (that is, $E_{NLRHA}$) for all the earthquakes. Each point on a scatterplot represents the comparison for a typical earthquake. The diagonal line across a scatterplot represents the ideal response (equivalent to a bias factor = 1). A point above this line represents an overestimation by the approximate method, and vice versa.

## 6. Observations and Discussions

The bias factor statistics summary in Tables 6 and 7 very clearly show that both proposed methods are able to estimate the hysteretic energy demand in asymmetric structures, albeit to a varying degree of accuracy depending on the building height and the degree of asymmetry. The mean bias is close to 1 and the CoV is small for most of the cases. This is

**TABLE 2** Some properties of the first three modal equivalent 2-DOF systems of the 9-story building with 10% eccentricity used in the 2D-MPA-based method

| Mode $n$ | $K_{xn}$ (kNm) | $\alpha_{xn}$ | $K_{\theta n}$ (kNm) | $\alpha_{\theta n}$ | $m$ (kNs$^2$/m) | $I_0$ (kNms$^2$) | $e$ (m) | $F_{yxn}$ (kN) | $F_{y\theta n}$ (kN) |
|---|---|---|---|---|---|---|---|---|---|
| 1 | 0.990 | 0.162 | 4.35E–02 | 0.220 | 173 | 1.69E–03 | –7.66E–04$^{\dagger}$ | 388 | 5.30 |
| 2 | 1.53E–02 | 0.347 | 2.87 | 0.763 | 2.62 | 0.111 | 4.92E–02 | 88.0 | 5740 |
| 3 | 7.04 | 0.148 | 0.316 | 0.177 | 172 | 1.74E–03 | –7.77E–04 | 1860 | 25.7 |

$^{\dagger}$A negative value of $e$ signifies that the point mass is located at the left of the roller support as per Fig. 1a.

**TABLE 3** Bias statistics for the 3-story building with 40% eccentricity for both the MPA-based and 2D-MPA-based methods

| Ground motion record | $E_{NLRHA}$ (kNm) | $E_{MPA}$ (kNm) | $E_{2D\text{-}MPA}$ (kNm) | $N_{MPA}$ | $N_{2D\text{-}MPA}$ |
|---|---|---|---|---|---|
| s549 | 6860 | 6290 | 7840 | 1.09 | 0.875 |
| s621 | 1660 | 1310 | 2130 | 1.27 | 0.782 |
| s640 | 1190 | 826 | 1490 | 1.43 | 0.795 |
| syl90 | 749 | 613 | 1650 | 1.22 | 0.454 |
| syl360 | 4220 | 3650 | 3030 | 1.16 | 1.40 |
| tcu0659 | 9740 | 9560 | 7670 | 1.02 | 1.27 |
| tcu06536 | 9950 | 9650 | 7850 | 1.03 | 1.27 |
| chy0809 | 7710 | 6160 | 5150 | 1.25 | 1.50 |
| chy08036 | 5040 | 4480 | 3490 | 1.12 | 1.44 |
| newh360 | 3870 | 3620 | 2900 | 1.07 | 1.34 |
| nh | 4220 | 3640 | 3000 | 1.16 | 1.41 |
| nr | 6790 | 6610 | 3830 | 1.03 | 1.77 |
| ns | 7120 | 6860 | 5000 | 1.04 | 1.42 |
| s050 | 5280 | 4910 | 4720 | 1.07 | 1.12 |
| s065 | 2290 | 1920 | 3080 | 1.19 | 0.744 |
| s212 | 3980 | 3260 | 6230 | 1.22 | 0.639 |
| s305 | 14000 | 13500 | 9350 | 1.04 | 1.50 |
| s503 | 643 | 213 | 2350 | 3.01 | 0.273 |
| | | | Mean | 1.25 | 1.11 |
| | | | SD | 0.455 | 0.418 |
| | | | CoV | 0.365 | 0.376 |
| | | | MaxEr (%) | 202 | 77.5 |



also evident from the scatterplots presented in Figs. 2–4. For the MPA-based method, the level of accuracy decreases as we go from the low-rise to the high-rise structures. Similar observations were noted in previous works on MPA [Chopra and Goel, 2004; Prasanth *et al.*, 2008]. An increase in the degree of asymmetry, as measured by the eccentricity, is not found to necessarily lower the accuracy level. However, for the 20-story structure, the mean bias (for the MPA-based method) drifts further away from its ideal value 1 as the eccentricity is increased. Overall, for the MPA-based method, the mean bias is found to be in the range of 1.20–1.86, which signifies that this method underestimates the hysteretic energy demand in the structure. This can also be observed for each specific earthquake in the scatterplots in Figs. 2–4. Prasanth *et al.* [2008] observed that the MPA-based method underestimates the hysteretic energy demand in symmetric structures, due to the fact that this method cannot incorporate the coupling of modes when the structure becomes inelastic. In addition to this, the MPA-based method for asymmetric structures suffers from the fact that the equivalent SDOF systems are based primarily on the translational behavior and the torsional behavior of the building is not directly included in these systems.

It is observed that for most of these cases, the contribution to $E_{MPA}$ is primarily from only the first mode. For many of the records, only the first mode contributes significantly. However, for a small number of records contributions from the other primarily translational modes are also significant. As an example, Table 9 provides mode-wise data for the 9-story

**TABLE 4** Bias statistics for the 9-story building with 10% eccentricity for both the MPA-based and 2D-MPA-based methods

| Ground motion record | $E_{NLRHA}$ (kNm) | $E_{MPA}$ (kNm) | $E_{2D\text{-}MPA}$ (kNm) | $N_{MPA}$ | $N_{2D\text{-}MPA}$ |
|---|---|---|---|---|---|
| s549 | 26100 | 25200 | 25700 | 1.04 | 1.02 |
| s621 | 4930 | 3540 | 4630 | 1.39 | 1.07 |
| s640 | 1470 | 583 | 1880 | 2.53 | 0.786 |
| syl90 | 7670 | 6540 | 6630 | 1.17 | 1.16 |
| syl360 | 12300 | 12200 | 11500 | 1.01 | 1.07 |
| tcu0659 | 25800 | 22300 | 25400 | 1.15 | 1.01 |
| tcu06536 | 16900 | 13100 | 17200 | 1.29 | 0.982 |
| chy0809 | 13700 | 11600 | 9880 | 1.18 | 1.38 |
| chy08036 | 10400 | 7620 | 7200 | 1.36 | 1.44 |
| newh360 | 4870 | 3740 | 5970 | 1.30 | 0.816 |
| nh | 12300 | 12100 | 11400 | 1.01 | 1.07 |
| nr | 11500 | 10900 | 11500 | 1.05 | 0.994 |
| ns | 14400 | 12100 | 13200 | 1.19 | 1.09 |
| s050 | 14900 | 13600 | 11900 | 1.10 | 1.26 |
| s065 | 3420 | 1980 | 5090 | 1.73 | 0.672 |
| s212 | 18600 | 15500 | 18500 | 1.20 | 1.01 |
| s305 | 28200 | 25600 | 20700 | 1.10 | 1.36 |
| s503 | 1990 | 868 | 3830 | 2.30 | 0.521 |
| | | | Mean | 1.34 | 1.04 |
| | | | SD | 0.428 | 0.239 |
| | | | CoV | 0.320 | 0.230 |
| | | | MaxEr (%) | 153 | 47.9 |



building with an eccentricity of 10%. As it can be observed here, there are a very few earthquake cases where the third mode, which is the second (primarily) translational mode, contributes more than the first mode. Similar observations, for these specific earthquake cases, were also reported by Prasanth *et al.* [2008] for symmetric building structures. As discussed in their article, these interesting results are attributed to the unique characteristics and frequency content of the input ground motion records. The primarily torsional modes do not significantly contribute to the energy demand as per the MPA-based method. The first primarily torsional mode contributes only for the 9- and 20-story buildings with larger eccentricities (30% and above), and only for a few of the earthquake records considered. Therefore one can neglect the primarily torsional modes in $E_h$ estimation using the MPA-based method, at least for the low-rise or low-eccentricity structures.

In the MPA-based method, the bias factor is observed to be higher in case of weak earthquakes. This is because of the fact that the difference between the original and the biliniearized pushover curves is the maximum around the point of yielding, which is the case for weak earthquakes. Plasticity begins in the original structure before the ESDOF system shows any plastic behaviour. Since the torsional behaviour is not properly accounted for in the ESDOF systems representing primarily translational modes (which contribute to the hysteretic energy demand), the demands on these ESDOF systems for weak earthquakes do not always reach the plastic zone resulting in $E_{MPA} \sim 0$, even though the actual structure already shows some plasticity. Figure 5 shows how the

**TABLE 5** Bias statistics for the 20-story building with 20% eccentricity for both the MPA-based and 2D-MPA-based methods

| Ground motion record | $E_{NLRHA}$ (kNm) | $E_{MPA}$ (kNm) | $E_{2D\text{-}MPA}$ (kNm) | $N_{MPA}$ | $N_{2D\text{-}MPA}$ |
|---|---|---|---|---|---|
| s549 | 26900 | 23500 | 25600 | 1.14 | 1.05 |
| s621 | 2360 | 1890 | 4180 | 1.25 | 0.564 |
| s640 | 2400 | 895 | 2290 | 2.68 | 1.05 |
| syl90 | 2200 | 1190 | 2790 | 1.85 | 0.790 |
| syl360 | 5050 | 3310 | 6100 | 1.52 | 0.828 |
| tcu0659 | 40800 | 39000 | 37600 | 1.05 | 1.09 |
| tcu06536 | 13500 | 8120 | 14500 | 1.67 | 0.932 |
| chy0809 | 4760 | 2620 | 6610 | 1.81 | 0.720 |
| chy08036 | 4140 | 1240 | 4940 | 3.34 | 0.838 |
| newh360 | 5230 | 2260 | 4840 | 2.32 | 1.08 |
| nh | 4950 | 3160 | 6000 | 1.57 | 0.824 |
| nr | 6780 | 4480 | 7300 | 1.51 | 0.928 |
| ns | 6020 | 3200 | 5510 | 1.88 | 1.09 |
| s050 | 12600 | 9420 | 12000 | 1.34 | 1.05 |
| s065 | 6290 | 3350 | 5700 | 1.88 | 1.10 |
| s212 | 15400 | 10200 | 16800 | 1.52 | 0.917 |
| s305 | 20300 | 16800 | 19000 | 1.21 | 1.07 |
| s503 | 6360 | 5210 | 6550 | 1.22 | 0.970 |
| | | | Mean | 1.71 | 0.938 |
| | | | SD | 0.582 | 0.152 |
| | | | CoV | 0.341 | 0.162 |
| | | | MaxEr (%) | 234 | 43.6 |

**TABLE 6** Summary of bias statistics for all the case studies using the MPA-based method

| | Eccentricity | | | | | |
|---|---|---|---|---|---|---|
| | 0% | 5% | 10% | 20% | 30% | 40% |
| 3-story | | | | | | |
| Mean | 1.20 | 1.22 | 1.26 | 1.25 | 1.20 | 1.25 |
| SD | 0.201 | 0.213 | 0.263 | 0.442 | 0.291 | 0.455 |
| CoV | 0.167 | 0.174 | 0.208 | 0.354 | 0.242 | 0.365 |
| MaxEr (%) | 55.3 | 58.0 | 83.9 | 187 | 115 | 202 |
| 9-story | | | | | | |
| Mean | 1.35 | 1.35 | 1.34 | 1.33 | 1.36 | 1.30 |
| SD | 0.499 | 0.472 | 0.428 | 0.396 | 0.379 | 0.306 |
| CoV | 0.370 | 0.351 | 0.320 | 0.298 | 0.279 | 0.235 |
| MaxEr (%) | 180 | 172 | 153 | 156 | 140 | 107 |
| 20-story | | | | | | |
| Mean | 1.43 | 1.46 | 1.51 | 1.71 | 1.86 | 1.84 |
| SD | 0.615 | 0.633 | 0.650 | 0.582 | 0.669 | 0.606 |
| CoV | 0.430 | 0.435 | 0.431 | 0.341 | 0.360 | 0.330 |
| MaxEr (%) | 255 | 265 | 278 | 234 | 250 | 219 |

**TABLE 7** Summary of bias statistics for all the case studies using the 2D-MPA-based method

| | Eccentricity | | | | |
|---|---|---|---|---|---|
| | 5% | 10% | 20% | 30% | 40% |
| 3-story | | | | | |
| Mean | 1.11 | 1.01 | 0.936 | 0.968 | 1.11 |
| SD | 0.127 | 0.203 | 0.303 | 0.300 | 0.418 |
| CoV | 0.115 | 0.202 | 0.323 | 0.310 | 0.376 |
| MaxEr (%) | 39.2 | 45.2 | 72.2 | 72.9 | 77.5 |
| 9-story | | | | | |
| Mean | 1.14 | 1.04 | 0.992 | 0.979 | 0.992 |
| SD | 0.148 | 0.239 | 0.267 | 0.307 | 0.375 |
| CoV | 0.130 | 0.230 | 0.269 | 0.313 | 0.378 |
| MaxEr (%) | 43.6 | 47.9 | 54.3 | 71.3 | 66.8 |
| 20-story | | | | | |
| Mean | 1.25 | 1.11 | 0.938 | 0.862 | 0.778 |
| SD | 0.274 | 0.127 | 0.152 | 0.214 | 0.294 |
| CoV | 0.218 | 0.114 | 0.162 | 0.249 | 0.377 |
| MaxEr (%) | 99.9 | 40.2 | 43.6 | 46.2 | 69.1 |

**TABLE 8** Mode-wise distribution of hysteretic energy demands for the 3-story building with 40% eccentricity as per the MPA-based method

| | $E_{nh}/E_{MPA}$ (where $E_{MPA} = \sum_{n=1}^{5} E_{nh}$) | | | | |
|---|---|---|---|---|---|
| Ground motion record | Mode 1 (%)[X] | Mode 2 (%)[R] | Mode 3 (%)[X] | Mode 4 (%)[X] | Mode 5 (%)[R] |
| s549 | 99.1 | 0 | 0.916 | 0 | 0 |
| s621 | 100 | 0 | 0 | 0 | 0 |
| s640 | 100 | 0 | 0 | 0 | 0 |
| syl90 | 100 | 0 | 0 | 0 | 0 |
| syl360 | 93.7 | 0 | 6.32 | 0 | 0 |
| tcu0659 | 100 | 0 | 0 | 0 | 0 |
| tcu06536 | 100 | 0 | 0 | 0 | 0 |
| chy0809 | 100 | 0 | 0 | 0 | 0 |
| chy08036 | 100 | 0 | 0 | 0 | 0 |
| newh360 | 100 | 0 | 0 | 0 | 0 |
| nh | 93.8 | 0 | 6.18 | 0 | 0 |
| nr | 100 | 0 | 0 | 0 | 0 |
| ns | 100 | 0 | 0 | 0 | 0 |
| s050 | 100 | 0 | 0 | 0 | 0 |
| s065 | 100 | 0 | 0 | 0 | 0 |
| s212 | 100 | 0 | 0 | 0 | 0 |
| s305 | 92.8 | 0.140 | 7.09 | 0 | 0 |
| s503 | 100 | 0 | 0 | 0 | 0 |

[X]Primarily translational mode.

[R]Primarily torsional mode.

**TABLE 9** Mode-wise distribution of hysteretic energy demands for the 9-story building with 10% eccentricity as per the MPA-based method

| Ground motion record | $E_{nh}/E_{MPA}$ (where $E_{MPA} = \sum_{n=1}^{5} E_{nh}$) | | | | |
|---|---|---|---|---|---|
| | Mode 1 (%)[X] | Mode 2 (%)[R] | Mode 3 (%)[X] | Mode 4 (%)[X] | Mode 5 (%)[R] |
| s549 | 87.7 | 0 | 12.3 | 0 | 0 |
| s621 | 100 | 0 | 0 | 0 | 0 |
| s640 | 100 | 0 | 0 | 0 | 0 |
| syl90 | 98.5 | 0 | 1.54 | 0 | 0 |
| syl360 | 100 | 0 | 0 | 0 | 0 |
| tcu0659 | 100 | 0 | 0 | 0 | 0 |
| tcu06536 | 99.4 | 0 | 0 | 0 | 0 |
| chy0809 | 34.7 | 0 | 65.3 | 0 | 0 |
| chy08036 | 31.5 | 0 | 68.5 | 0 | 0 |
| newh360 | 76.0 | 0 | 24.0 | 0 | 0 |
| nh | 100 | 0 | 0 | 0 | 0 |
| nr | 75.4 | 0 | 24.6 | 0 | 0 |
| ns | 72.4 | 0 | 27.6 | 0 | 0 |
| s050 | 100 | 0 | 0 | 0 | 0 |
| s065 | 100 | 0 | 0 | 0 | 0 |
| s212 | 100 | 0 | 0 | 0 | 0 |
| s305 | 89.8 | 0 | 10.2 | 0 | 0 |
| s503 | 100 | 0 | 0 | 0 | 0 |

[X]Primarily translational mode.
[R]Primarily torsional mode.



MPA-based estimations, on average, get better for stronger earthquakes (that is when the $E_{NLRHA}$ is high) for the 9-story structure with different eccentricity values. Similar trend is also observed for 3- and 20-story structures [Rathore, 2009]. No such behavior is observed in the case of the 2D-MPA-based method since it directly accounts for the torsional behaviour in its 2-DOF equivalent systems. Figure 6 presents the variations of $N_{2D\text{-}MPA}$ with the actual energy demand for the 9-story structure with different eccentricity values. It should be noted that the hysteretic energy-based design approach is aimed at designing for cases where there is significant $E_{NLRHA}$ and not when the structural behavior is at the borderline of elastic and inelastic behavior.

The level of accuracy for the 2D-MPA-based estimations, overall, is significantly better than that of the MPA-based estimations. The mean bias values, ranging from 0.806–1.25, are closer to 1 for the 2D-MPA-based method. In general, the scatter (measured by CoV) is also lower for this method. Although the estimations are best for the 3-story building (similar to the MPA-based method), there is no significant decrease in the accuracy level for the 9- and 20-story buildings. Unlike the MPA-based method, there is no significant trend of overestimation or underestimation by the 2D-MPA-based method, although there is a weak trend of overestimation for buildings with higher eccentricity. The better performance of the 2D-MPA-based method can be attributed to the fact that the 2-DOF equivalent systems directly incorporate the torsional effects in the original building along with the translational. There exists the hysteretic energy

**TABLE 10** Mode-wise distribution of hysteretic energy demands for the 20-story building with 20% eccentricity as per the MPA-based method

| Ground motion record | $E_{nh}/E_{MPA}$ (where $E_{MPA} = \sum_{n=1}^{5} E_{nh}$) Mode 1 (%)$^{X}$ | Mode 2 (%)$^{R}$ | Mode 3 (%)$^{X}$ | Mode 4 (%)$^{X}$ | Mode 5 (%)$^{R}$ |
|---|---|---|---|---|---|
| s549 | 98.9 | 0 | 1.08 | 0 | 0 |
| s621 | 100 | 0 | 0 | 0 | 0 |
| s640 | 100 | 0 | 0 | 0 | 0 |
| syl90 | 100 | 0 | 0 | 0 | 0 |
| syl360 | 100 | 0 | 0 | 0 | 0 |
| tcu0659 | 99.8 | 0 | 0.169 | 0 | 0 |
| tcu06536 | 100 | 0 | 0 | 0 | 0 |
| chy0809 | 0 | 0 | 100 | 0 | 0 |
| chy08036 | 0 | 0 | 100 | 0 | 0 |
| newh360 | 76.8 | 0 | 23.2 | 0 | 0 |
| nh | 100 | 0 | 0 | 0 | 0 |
| nr | 54.2 | 0 | 45.7 | 0 | 0 |
| ns | 34.2 | 0 | 65.8 | 0 | 0 |
| s050 | 99.8 | 0 | 0.199 | 0 | 0 |
| s065 | 100 | 0 | 0 | 0 | 0 |
| s212 | 100 | 0 | 0 | 0 | 0 |
| s305 | 73.8 | 0 | 26.2 | 0 | 0 |
| s503 | 100 | 0 | 0 | 0 | 0 |

$^{X}$Primarily translational mode.
$^{R}$Primarily torsional mode.

contribution from the spring representing the torsional behavior, in addition to what is observed in the MPA-based method. This increase in the energy estimated by the 2D-MPA-based method due to the contribution from the "torsional spring" lowers the bias factor, sometimes causing an overestimation. In cases with higher eccentricity, the contribution from this spring is increased, which may be the reason for that weak trend of overestimation. The eccentricity is only one parameter alongside several others, such as modal frequencies, that determine a building's dynamic behavior for a selected ground motion. For example, with an increase in the eccentricity of a building, the time period for a primarily translational mode increases, while that of a primarily torsional mode reduces, changing the inelastic coupling between the two modes. Thus, no robust trends are observed for a change in the eccentricity while using the 2D-MPA-based method. The increase in the level of accuracy by using the 2D-MPA-based method, in place of the MPA-based method, for energy demand estimation, comes at a cost of significant increase in the complexity in the formulation of the equivalent systems. Results from these case studies indicate where there is a significant advantage (in terms of closeness to the NLRHA results) in using 2D-MPA-based method instead of the MPA-based method, even at increased complexity.

It should be noted that the primarily torsional modes do not contribute at all to the hysteretic energy demand using the 2D-MPA-based method. The contribution of an equivalent system corresponding to a torsional mode should not be confused with the

**TABLE 11** Mode-wise distribution of hysteretic energy demands for the 3-story building with 40% eccentricity as per the 2D-MPA-based method

| Ground motion record | $E_{nh}/E_{2D\text{-}MPA}$ (where $E_{2D-MPA} = \sum_{n=1}^{5} E_{nh}$) | | | | |
|---|---|---|---|---|---|
| | Mode 1 (%)[X] | Mode 2 (%)[R] | Mode 3 (%)[X] | Mode 4 (%)[X] | Mode 5 (%)[R] |
| s549 | 93.6 | 0 | 6.43 | 0 | 0 |
| s621 | 93.3 | 0 | 6.65 | 0 | 0 |
| s640 | 89.8 | 0 | 10.2 | 0 | 0 |
| syl90 | 96.7 | 0 | 3.32 | 0 | 0 |
| syl360 | 89.5 | 0 | 10.5 | 0 | 0 |
| tcu0659 | 99.5 | 0 | 0.467 | 0 | 0 |
| tcu06536 | 99.9 | 0 | 0.111 | 0 | 0 |
| chy0809 | 94.9 | 0 | 5.08 | 0 | 0 |
| chy08036 | 94.8 | 0 | 5.18 | 0 | 0 |
| newh360 | 92.7 | 0 | 7.33 | 0 | 0 |
| nh | 89.4 | 0 | 10.6 | 0 | 0 |
| nr | 90.3 | 0 | 9.71 | 0 | 0 |
| ns | 98.1 | 0 | 1.92 | 0 | 0 |
| s050 | 97.9 | 0 | 2.07 | 0 | 0 |
| s065 | 95.5 | 0 | 4.49 | 0 | 0 |
| s212 | 99.6 | 0 | 0.427 | 0 | 0 |
| s305 | 78.4 | 0 | 21.6 | 0 | 0 |
| s503 | 99.8 | 0 | 0.231 | 0 | 0 |

[X]Primarily translational mode.
[R]Primarily torsional mode.



contribution from the torsional spring of the equivalent 2-DOF system corresponding to a primarily translational mode. The primarily torsional modes do not contribute as no inelastic activity takes place in these modes. The torsional modes, however, contribute to elastic parameters or parameters with elastic components, such as roof displacement [Rathore, 2009; Lin and Tsai, 2007].

In general, for both the approximate methods, the difference between the original pushover curve and the bilinear approximation also introduces some error in estimating the hysteretic energy demand. For example, for large structures with more possible plastic hinge locations, the pushover curve changes from elastic to almost fully plastic very gradually, and this is very different from the bilinear approximation. Therefore, it is more likely to have an erroneous result for a taller structure than for a smaller low-rise building where the original pushover curve is close to the approximating bilinear curve.

## 7. A Sample Case Study for a Torsionally Flexible Structure

The buildings discussed in the previous two sections, even with eccentricities as high as 40%, can be termed as "torsionally stiff" structures, based on the $I_0/m$ ratio for each floor, as per Chopra and Goel [2004]. In other words, a structure can be considered to be torsionally stiff if the time period of its first primarily translational mode is significantly longer than that of the first primarily torsional mode. It is expected for such buildings to

**TABLE 12** Mode-wise distribution of hysteretic energy demands for the 9-story building with 10% eccentricity as per the 2D-MPA-based method

| | $E_{nh}/E_{2D\text{-}MPA}$ (where $E_{2D-MPA} = \sum_{n=1}^{5} E_{nh}$) | | | | |
|---|---|---|---|---|---|
| Ground motion record | Mode 1 (%)[X] | Mode 2 (%)[R] | Mode 3 (%)[X] | Mode 4 (%)[X] | Mode 5 (%)[R] |
| s549 | 90.7 | 0 | 9.33 | 0 | 0 |
| s621 | 91.1 | 0 | 8.94 | 0 | 0 |
| s640 | 87.3 | 0 | 12.7 | 0 | 0 |
| syl90 | 92.2 | 0 | 7.82 | 0 | 0 |
| syl360 | 97.7 | 0 | 2.28 | 0 | 0 |
| tcu0659 | 95.9 | 0 | 4.11 | 0 | 0 |
| tcu06536 | 91.7 | 0 | 8.29 | 0 | 0 |
| chy0809 | 50.2 | 0 | 49.8 | 0 | 0 |
| chy08036 | 50.2 | 0 | 49.8 | 0 | 0 |
| newh360 | 77.5 | 0 | 22.5 | 0 | 0 |
| nh | 97.7 | 0 | 2.29 | 0 | 0 |
| nr | 74.2 | 0 | 25.8 | 0 | 0 |
| ns | 81.8 | 0 | 18.2 | 0 | 0 |
| s050 | 96.5 | 0 | 3.49 | 0 | 0 |
| s065 | 89.6 | 0 | 10.4 | 0 | 0 |
| s212 | 96.1 | 0 | 3.90 | 0 | 0 |
| s305 | 85.1 | 0 | 14.9 | 0 | 0 |
| s503 | 95.0 | 0 | 5.01 | 0 | 0 |

[X]Primarily translational mode.
[R]Primarily torsional mode.

have very low to moderate torsional behaviour. The proposed methods need to be checked for "torsionally flexible" and "torsionally equally flexible" structures as well. In this section, the application of the proposed methods on a torsionally flexible structure is discussed. The study structure is considered to be torsionally flexible because its fundamental mode of vibration is primarily rotational and the natural period for the first primarily translational mode is shorter than that.

The torsionally flexible structure is obtained by artificially increasing the $I_0$ at each floor 3.5 times, without changing the floor mass ($m$), for the 3-story building with 5% mass eccentricity which was considered in Secs. 5–6. This increase in the rotational inertia shifts the first two time periods from 1.00 s (translational) and 0.598 s (rotational) to 1.13 s (rotational) and 0.989 s (translational). Both the proposed methods are applied to this structure for the same set of earthquakes considered earlier, and the results for each earthquake with bias data are presented in Table 14. Both the methods are found to be effective in estimating the hysteretic energy demand of this torsionally flexible structure. However, based on the statistics of mean, SD and CoV, the levels of accuracy are lower for both the methods when compared to the corresponding torsionally stiff structure considered earlier. Tables 15 and 16 show that the first primarily torsional mode contributes to the total energy demand for many earthquake cases. It should be restated here that for torsionally stiff structures, the 2D-MPA-based method does not show any contribution from the primarily torsional modes, and the MPA-based method does not show any such contribution other than high-rise structures with

**TABLE 13** Mode-wise distribution of hysteretic energy demands for the 20-story building with 20% eccentricity as per the 2D-MPA-based method

| | $E_{nh}/E_{2D\text{-}MPA}$ (where $E_{2D-MPA} = \sum_{n=1}^{5} E_{nh}$) | | | | |
|---|---|---|---|---|---|
| Ground motion record | Mode 1 (%)[X] | Mode 2 (%)[R] | Mode 3 (%)[X] | Mode 4 (%)[X] | Mode 5 (%)[R] |
| s549 | 88.5 | 0 | 9.67 | 1.82 | 0 |
| s621 | 88.5 | 0 | 11.2 | 0.303 | 0 |
| s640 | 84.4 | 0 | 14.7 | 0.854 | 0 |
| syl90 | 88.1 | 0 | 11.6 | 0.333 | 0 |
| syl360 | 77.6 | 0 | 21.0 | 1.03 | 0 |
| tcu0659 | 89.5 | 0 | 10.4 | 0 | 0 |
| tcu06536 | 73.1 | 0 | 25.9 | 1.03 | 0 |
| chy0809 | 7.48 | 0 | 75.0 | 17.3 | 0 |
| chy08036 | 28.3 | 0 | 60.5 | 11.1 | 0 |
| newh360 | 51.4 | 0 | 38.5 | 10.0 | 0 |
| nh | 77.3 | 0 | 21.3 | 1.03 | 0 |
| nr | 47.8 | 0 | 44.1 | 7.89 | 0 |
| ns | 19.5 | 0 | 73.9 | 6.57 | 0 |
| s050 | 84.4 | 0 | 15.5 | 0.126 | 0 |
| s065 | 81.1 | 0 | 18.9 | 0 | 0 |
| s212 | 92.0 | 0 | 7.95 | 0 | 0 |
| s305 | 67.6 | 0 | 27.7 | 4.08 | 0 |
| s503 | 97.6 | 0 | 2.36 | 0 | 0 |

[X]Primarily translational mode.
[R]Primarily torsional mode.



large eccentricity. The torsional mode shows hysteretic energy demands for the torsionally flexible structure because there is some inelastic activity—unlike for the torsionally stiff structures—associated with this mode.

Therefore, one needs to revisit the general recommendation from Sec. 6 of not including the torsional modes in calculation (excluding high-rise and large-eccentricity structures in MPA-based method). Based on this sample case study, the first primarily torsional mode needs to be included for the energy demand estimation for torsionally flexible structures for both the proposed methods. It is expected that the contribution from this mode will be more significant for high-rises with larger eccentricity.

## 8. Summary and Conclusions

This article proposes an MPA-based and a 2D-MPA-based approximate method to estimate hysteretic energy demand in plan-asymmetric buildings structures. The primary focus of this work is in checking the effectiveness of the proposed methods for low-to-high-rise asymmetric buildings and for a wide range of plan eccentricity values subjected to a large set of strong motion records. The emphasis is on the application of the proposed methods to torsionally stiff structures, although a sample study on a torsionally flexible structure is considered. The bias factor statistics generated here can be incorporated in a probability-based design method considering hysteretic energy demand, as illustrated by

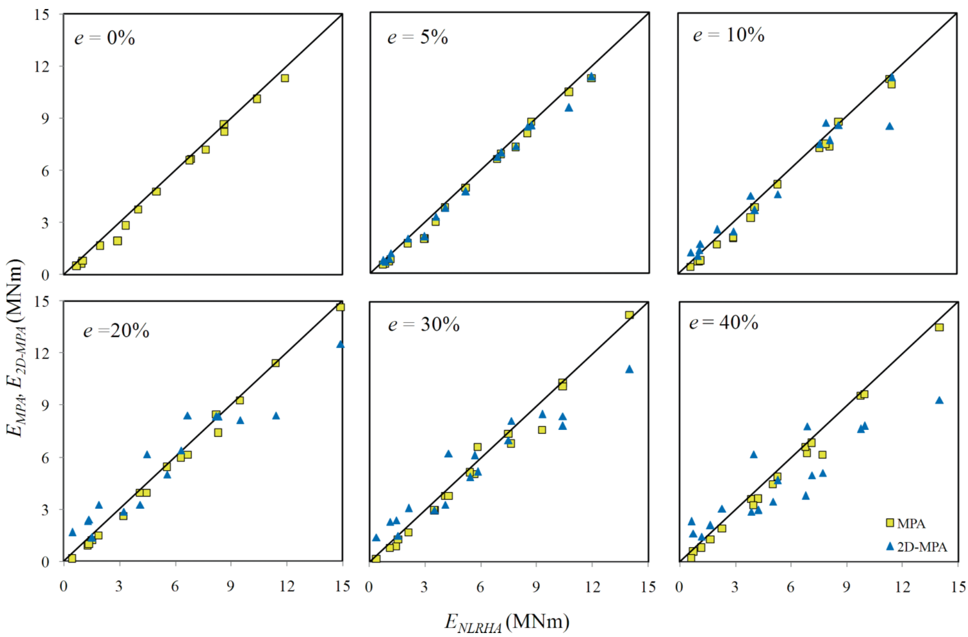


**FIGURE 2** Scatterplots comparing $E_{MPA}$ and $E_{2D\text{-}MPA}$ with $E_{NLRHA}$ for the 3-story structures. (Figure is provided in color online.)

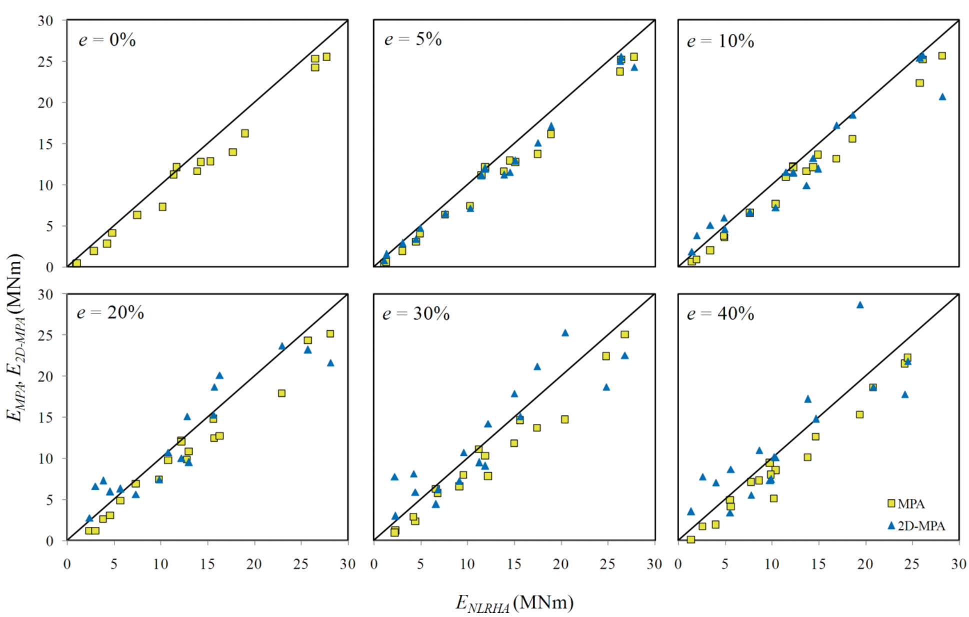


**FIGURE 3** Scatterplots comparing $E_{MPA}$ and $E_{2D\text{-}MPA}$ with $E_{NLRHA}$ for the 9-story structures. (Figure is provided in color online.)

Ghosh and Collins [2006] where the bias statistics were used to obtain the partial safety factors in the energy-based design checking equation in a reliability-based framework. For deterministic methods, the mean bias can be used as a correction factor while estimating the hysteretic energy demand using the proposed approximate procedures.

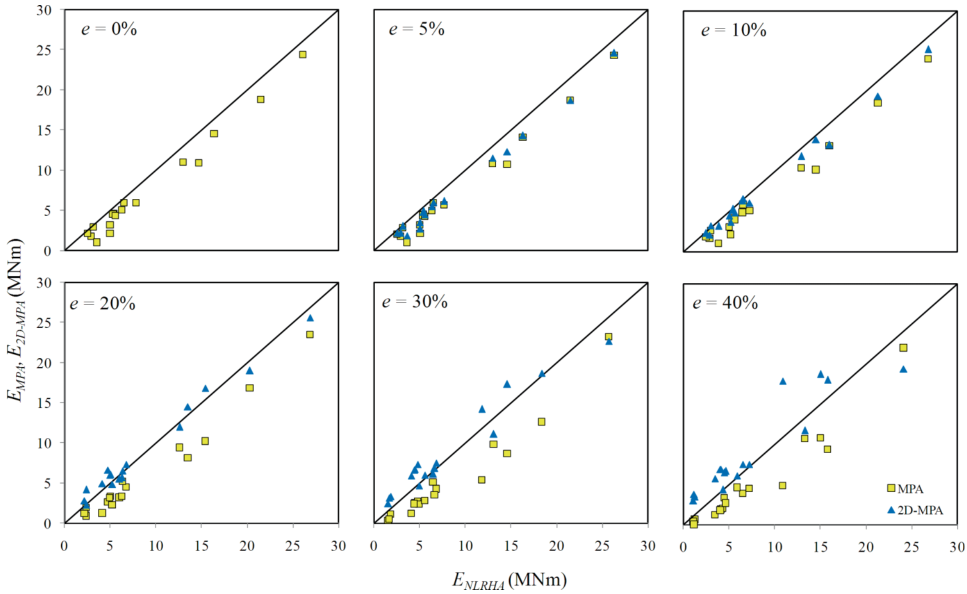


**FIGURE 4** Scatterplots comparing $E_{MPA}$ and $E_{2D\text{-}MPA}$ with $E_{NLRHA}$ for the 20-story structures. (Figure is provided in color online.)

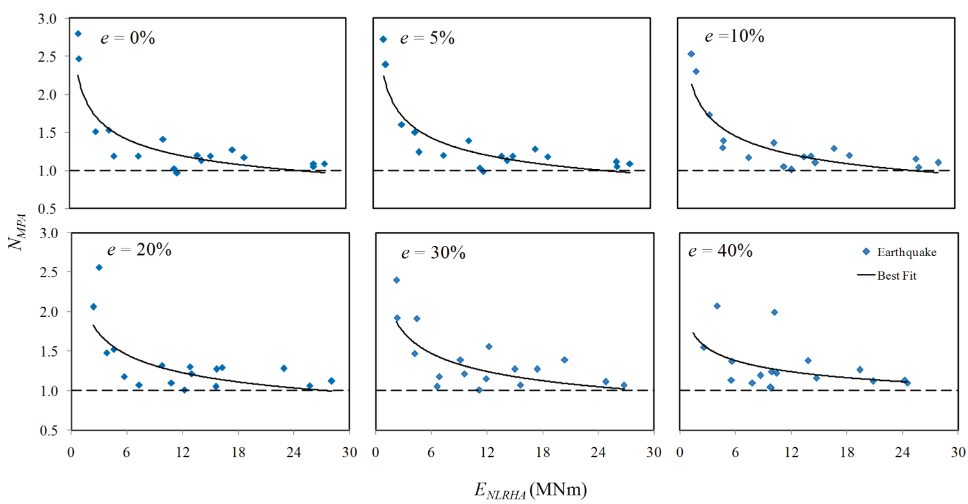


**FIGURE 5** Variation of bias factor ($N_{MPA}$) with actual hysteretic energy demand ($E_{NLRHA}$) for the 9-story structures. (Figure is provided in color online.)

These methods, thus, can be utilized for both the energy-based design and performance assessment of structures.

The following general conclusions are drawn based on application case studies of the MPA-based and 2D-MPA-based approximate methods of hysteretic energy demand:

- The proposed procedures remain simple and computationally efficient methods of estimating hysteretic energy demand on asymmetric structures.
- The MPA-based method generally underestimates the hysteretic energy demand with the level of accuracy decreasing with increasing building height and increasing

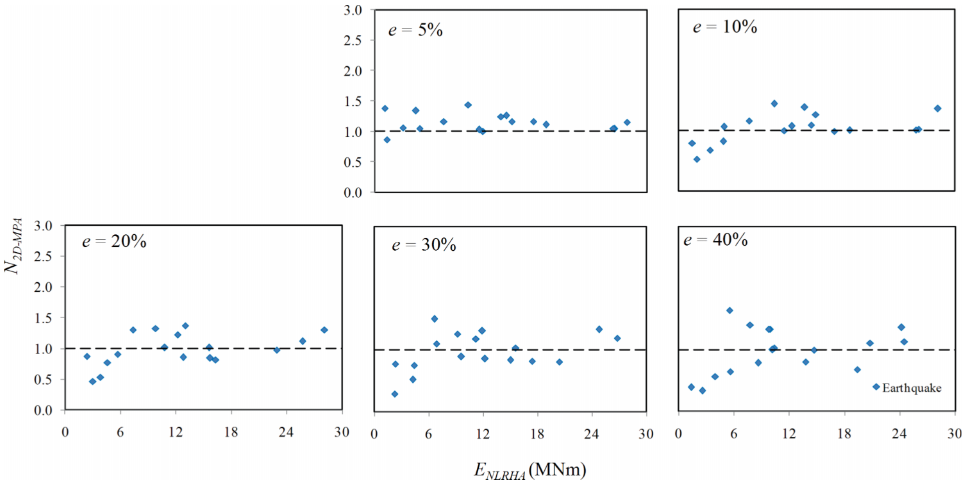


**FIGURE 6** Variation of bias factor ($N_{2D\text{-}MPA}$) with actual hysteretic energy demand ($E_{NLRHA}$) for the 9-story structures. (Figure is provided in color online.)

**TABLE 14** Bias statistics for the 3-story torsionally flexible building for both the MPA-based and 2D-MPA-based methods

| Ground motion record | $E_{NLRHA}$ (kNm) | $E_{MPA}$ (kNm) | $E_{2D\text{-}MPA}$ (kNm) | $N_{MPA}$ | $N_{2D\text{-}MPA}$ |
|---|---|---|---|---|---|
| s549 | 7520 | 6430 | 6430 | 1.17 | 1.22 |
| s621 | 901 | 498 | 695 | 1.81 | 1.48 |
| s640 | 656 | 300 | 539 | 2.19 | 1.48 |
| syl90 | 736 | 503 | 481 | 1.46 | 1.44 |
| syl360 | 2880 | 1700 | 1710 | 1.69 | 1.71 |
| tcu0659 | 9580 | 8420 | 9520 | 1.14 | 1.13 |
| tcu06536 | 6650 | 5720 | 6320 | 1.16 | 1.12 |
| chy0809 | 11700 | 10700 | 10500 | 1.09 | 1.13 |
| chy08036 | 8650 | 7920 | 7330 | 1.09 | 1.15 |
| newh360 | 3950 | 3440 | 3380 | 1.15 | 1.20 |
| nh | 2870 | 1700 | 1710 | 1.69 | 1.70 |
| nr | 6710 | 6300 | 5880 | 1.07 | 1.16 |
| ns | 8540 | 8230 | 7850 | 1.04 | 1.11 |
| s050 | 4770 | 3960 | 4520 | 1.20 | 1.13 |
| s065 | 1960 | 1490 | 1750 | 1.32 | 1.16 |
| s212 | 3150 | 2220 | 3000 | 1.42 | 1.17 |
| s305 | 15800 | 12900 | 12600 | 1.23 | 1.28 |
| s503 | 1020 | 690 | 897 | 1.48 | 1.23 |
| | | | Mean | 1.35 | 1.28 |
| | | | SD | 0.314 | 0.197 |
| | | | CoV | 0.232 | 0.154 |
| | | | MaxEr (%) | 119 | 71.0 |

**TABLE 15** Mode-wise distribution of hysteretic energy demands for the 3-story torsionally flexible building as per the MPA-based method

| | $E_{nh}/E_{2D\text{-}MPA}$ (where $E_{2D-MPA} = \sum_{n=1}^{5} E_{nh}$) | | | | |
|---|---|---|---|---|---|
| Ground motion record | Mode 1 (%)[R] | Mode 2 (%)[X] | Mode 3 (%)[R] | Mode 4 (%)[X] | Mode 5 (%)[R] |
| s549 | 0 | 100 | 0 | 0 | 0 |
| s621 | 0 | 100 | 0 | 0 | 0 |
| s640 | 0 | 100 | 0 | 0 | 0 |
| syl90 | 0 | 100 | 0 | 0 | 0 |
| syl360 | 0 | 100 | 0 | 0 | 0 |
| tcu0659 | 0 | 100 | 0 | 0 | 0 |
| tcu06536 | 0 | 100 | 0 | 0 | 0 |
| chy0809 | 2.38 | 97.6 | 0 | 0 | 0 |
| chy08036 | 0 | 100 | 0 | 0 | 0 |
| newh360 | 0 | 100 | 0 | 0 | 0 |
| nh | 0 | 100 | 0 | 0 | 0 |
| nr | 1.42 | 98.6 | 0 | 0 | 0 |
| ns | 3.54 | 96.5 | 0 | 0 | 0 |
| s050 | 0 | 100 | 0 | 0 | 0 |
| s065 | 0 | 100 | 0 | 0 | 0 |
| s212 | 0 | 100 | 0 | 0 | 0 |
| s305 | 1.14 | 95.7 | 0 | 3.19 | 0 |
| s503 | 0 | 100 | 0 | 0 | 0 |

[X]Primarily translational mode.
[R]Primarily torsional mode.

eccentricity (mean bias ranges from 1.20–1.86 for different heights and plan-eccentricity of a building).

- The 2D-MPA-based method gives significantly better estimates than the MPA-based method, with no significant trend of underestimation or overestimation (mean bias ranges from 0.778–1.25 for different heights and plan-eccentricity of a building). The level of accuracy does not change much with changing building height and degree of asymmetry.
- Although the 2D-MPA-based method gives better estimates, its formulation is more complex than the MPA-based method and it cannot utilize a response spectrum directly, since it uses 2-DOF equivalent systems. The MPA-based method can be easily incorporated in a response-spectrum based design or evaluation approach.
- For the MPA-based method, the degree of accuracy improves where the actual energy demand is high, while no such trend is observed for the 2D-MPA-based estimates.
- For both the methods, considering the first three primarily translational modes is sufficient for hysteretic energy demand estimation on torsionally stiff structures. For high-rise buildings with large plan eccentricity, the MPA-based method requires the inclusion of the first primarily torsional mode as well.
- For torsionally flexible structures, the first primarily torsional mode needs to be included, along with the first two translational modes, for both the methods.

**TABLE 16** Mode-wise distribution of hysteretic energy demands for the 3-story torsionally flexible building as per the 2D-MPA-based method

| | $E_{nh}/E_{2D\text{-}MPA}$ (where $E_{2D-MPA} = \sum_{n=1}^{5} E_{nh}$) | | | | |
|---|---|---|---|---|---|
| Ground motion record | Mode 1 (%)$^R$ | Mode 2 (%)$^X$ | Mode 3 (%)$^R$ | Mode 4 (%)$^X$ | Mode 5 (%)$^R$ |
| s549 | 0 | 100 | 0 | 0 | 0 |
| s621 | 0 | 100 | 0 | 0 | 0 |
| s640 | 0 | 100 | 0 | 0 | 0 |
| syl90 | 0 | 100 | 0 | 0 | 0 |
| syl360 | 0 | 99.7 | 0 | 0.281 | 0 |
| tcu0659 | 0 | 100 | 0 | 0 | 0 |
| tcu06536 | 0 | 100 | 0 | 0 | 0 |
| chy0809 | 0.283 | 99.7 | 0 | 0 | 0 |
| chy08036 | 0.724 | 99.3 | 0 | 0 | 0 |
| newh360 | 0 | 100 | 0 | 0 | 0 |
| nh | 0 | 99.7 | 0 | 0.287 | 0 |
| nr | 0.355 | 99.6 | 0 | 0 | 0 |
| ns | 0.205 | 99.8 | 0 | 0 | 0 |
| s050 | 0 | 100 | 0 | 0 | 0 |
| s065 | 0 | 100 | 0 | 0 | 0 |
| s212 | 0 | 100 | 0 | 0 | 0 |
| s305 | 0 | 98.3 | 0 | 1.67 | 0 |
| s503 | 0 | 100 | 0 | 0 | 0 |

$^X$Primarily translational mode.
$^R$Primarily torsional mode.

The proposed methods need to be checked thoroughly for asymmetric buildings that are categorized under "torsionally flexible" and "torsionally equally flexible" structures. Also, they need to be checked for degrading/pinched hysteretic behavior, other building configurations (such as braced frames, shear walls, etc.), and for the inclusion of geometric nonlinearity [Roy Chowdhury and Ghosh, 2007]. The study presented here is based on energy estimation at the global level only, whereas the energy demand at each plastic hinge location is of more importance. An extension of the current work on the estimation of local energy demands is already taken up by this research group. In addition, future extension of the proposed work can be in the line of the 3D-MPA method [Lin and Tsai, 2008] for energy demand estimation in biaxial plan-asymmetric buildings.

## References

Charney, F. A. [1999] *NONLIN (Nonlinear Dynamic Time History Analysis of Single Degree of Freedom Systems) User's Manual*, Advanced Structural Concepts, Inc., Blacksburg, Virginia.

Chopra, A. K. and Goel, R. K. [2002] "A modal pushover analysis procedure for estimating seismic demands for buildings," *Earthquake Engineering and Structural Dynamics* **31**(3), 561–582.

Chopra, A. K. and Goel, R. K. [2004] "A modal pushover analysis procedure to estimate seismic demands for unsymmetric-plan buildings," *Earthquake Engineering and Structural Dynamics* **33**(8), 903–927.

Erberik, A. and Sucuoğlu, H. [2004] "Seismic energy dissipation in deteriorating systems through low-cycle fatigue," *Earthquake Engineering and Structural Dynamics* **33**(1), 49–67.

Fajfar, P. [1992] "Equivalent ductility factors, taking into account low-cycle fatigue," *Earthquake Engineering and Structural Dynamics* **21**(10), 837–848.

Fajfar, P. and Gašperešič, P. [1996] "The N2 method for the seismic damage analysis of RC buildings," *Earthquake Engineering and Structural Dynamics* **25**(1), 31–46.

Ghosh, S. [2003] "Two alternatives for implementing performance-based seismic design of buildings—life cycle cost and seismic energy demand," Ph.D. thesis, Department of Civil and Environmental Engineering, University of Michigan, Ann Arbor, Michigan.

Ghosh, S. and Collins, K. R. [2006] "Merging energy-based design criteria and reliability-based methods: exploring a new concept," *Earthquake Engineering and Structural Dynamics* **35**(13), 1677–1698.

Gupta, A. and Krawinkler, H. [1999] "Seismic demands for performance evaluation of steel moment resisting frame structures (SAC task 5.4.3)," *Report No. 132*, John A. Blume Earthquake Engineering Center, Department of Civil and Environmental Engineering, Stanford University, Stanford, California.

Housner, G. W. [1956] "Limit design of structures to resist earthquakes," *Proc. of the First World Conference of Earthquake Engineering*, EERI, Berkeley, California.

Kunnath, S. K., Mander, J. B., and Fang, L. [1997] "Parameter identification for degrading and pinched hysteretic structural concrete systems," *Engineering Structures* **19**(3), 224–232.

Lin, J.-L. and Tsai, K.-C. [2007] "Simplified seismic analysis of asymmetric building systems," *Earthquake Engineering and Structural Dynamics* **36**(4), 459–479.

Lin, J.-L. and Tsai, K.-C. [2008] "Seismic analysis of two-way asymmetric building systems under bi-directional seismic ground motions," *Earthquake Engineering and Structural Dynamics* **37**(2), 305–325.

Manfredi, G. [2001] "Evaluation of seismic energy demand," *Earthquake Engineering and Structural Dynamics* **30**(4), 485–499.

Mazzoni, S., McKenna, F., Scott, M. H, Fenves, G. L., and Jeremic, B. [2007] *Open System for Earthquake Engineering Simulation (OpenSees) Command Language Manual*, University of California, Berkeley, California.

Prakash, V., Powell, G. H. and Campbell, S. [1993] "DRAIN-2DX base program description and user guide, version 1.10.," *Report No. UCB/SEMM-93/17*, University of California at Berkeley, California.

Prasanth, T., Ghosh, S., and Collins, K. R. [2008] "Estimation of hysteretic energy demand using concepts of modal pushover analysis," *Earthquake Engineering and Structural Dynamics* **37**(6), 975–990.

Rathore, M. [2009] "Estimation of hysteretic energy demand using MPA and 2D-MPA based methods for uniaxial plan-asymmetric structures," M.Tech. thesis, Department of Civil Engineering, Indian Institute of Technology Bombay, Mumbai, India.

Roy Chowdhury, A. and Ghosh, S. [2007] "Estimation of hysteretic energy demand including P-Delta effect using equivalent systems," *Proc. of the International Workshop on Earthquake Hazards and Mitigation*, Guwahati, India, December 6–8.

Structural Engineers Association of California (SEAOC) VISION 2000 Committee [1995] *Performance Based Seismic Engineering of Buildings: Vol. 1*, SEAOC, Sacramento, California.

Uang, C. M., Bertero, V. V. [1988] "Use of energy as a design criterion in earthquake-resistant design," *Report No. UCB/EERC- 88/18*, University of California, Berkeley, California.

Zahra, T. F. and Hall, W. J. [1984] "Earthquake energy absorption in SDOF structures," *Journal of Structural Engineering, ASCE* **110**(8), 1757–1772.